Influence of Hydrostatic Approximation on Coastal Current Simulation

Yasuo Nihei[1], Yusuke Yamasaki[1], Kazuo Nadaoka[2] and Tsukasa Nishimura[1]

1) Department of Civil Engineering, Tokyo University of Science, Noda, Chiba, Japan
2) Department of Mechanical and Environmental Informatics, Tokyo Institute of Technology, Meguro, Tokyo, Japan

ABSTRACT

To examine the influences of a hydrostatic approximation on the numerical accuracy of coastal current simulations, we have performed the computation for a vertical 2-D density front under a wide range of grid resolutions. For this purpose, we use the numerical models with and without the hydrostatic approximation. The computational results indicate that the differences of density-front structures appear appreciably in the hydrostatic and non-hydrostatic models and furthermore are strongly dependent on the horizontal grid resolutions. It is also found that the evaluation of a hydrodynamic pressure is a crucial importance on the numerical accuracy in the non-hydrostatic model.

KEY WORDS: Hydrostatic approximation; non-hydrostatic model; coastal current simulation; density front; grid resolution.

INTRODUCTION

Although coastal current simulations have frequently been performed in various flow fields, numerical models for coastal ocean current are usually based on several simplifications and approximations for turbulence models, coordinate systems, vertical fluid motion and etc (*e*.g., Haidvogel and Beckmann, 1998). It is therefore required to examine the influence of these simplifications on coastal current simulations. In most numerical models, the hydrostatic approximation, one of these simplifications in numerical models, is used for a vertical fluid motion (*e*.g., Blumberg and Mellor, 1983), because a horizontal length scale of fluid motion is much larger than a vertical length scale. However the coastal currents in which the vertical fluid motion is important exist such as coastal fronts, and hence we need to understand the influence of the hydrostatic approximation on coastal current simulations. Although previous studies have been conducted for this purpose (*e*.g., Causulli & Stelling, 1999; Kinoshita, 2001), the numerical accuracy of the hydrostatic approximation under a variety of computational conditions has been poorly investigated.

In the present study, we have attempted to study the influences of the hydrostatic approximation on computational results of coastal current simulations. For this purpose, we have done the computations for a vertical 2-dimensional gravity front, so called 'lock exchange problem' (Turner, 1973) under a wide range of grid resolutions by using numerical models for coastal current with and without the hydrostatic approximation.

COMPUTATIONAL METHOD

Outline of present method

To clarify the computational performance of the hydrostatic approximation in coastal current simulations, in the present study, we employ two numerical models for coastal current simulations with and without the hydrostatic approximation. The 3D numerical models with and without the hydrostatic approximation used here are referred to as 'hydrostatic model' and 'non-hydrostatic model', respectively. In the hydrostatic model, the governing equations are composed of the conservation of mass and momentum in the horizontal direction, and then the vertical velocity is evaluated with the continuity equation. On the other hand, in the non-hydrostatic model, we adopt the horizontal and vertical momentum equations and the Poisson equation for a pressure. Both the numerical models are based on the Boussinesq approximation, a sigma-coordinate system (Philips, 1957) and the smagorinsky model as a turbulence model. For reducing computational load, we apply a mode splitting technique, which divides the flow into baroclinic and barotropic (vertically averaged) modes. It should be noted that, for numerical accuracy, the pressure in the non-hydrostatic model is separated into hydrostatic and hydrodynamic pressure components, p_s and p_d, respectively, the latter being calculated with the Poisson equation.

Governing equations
We shall outline the governing equations in the hydrostatic and non-hydrostatic models in the following. In the hydrostatic model, we adopt the continuity and horizontal momentum equations as given by

$$\frac{\partial u}{\partial x} + \frac{\partial v}{\partial y} + \frac{1}{D}\frac{\partial w}{\partial s} + \frac{1}{D}\frac{\partial D}{\partial t} = 0 , \qquad (1)$$

$$\frac{\partial u}{\partial t}+u\frac{\partial u}{\partial x}+v\frac{\partial u}{\partial y}+w\frac{\partial u}{\partial z}-fv = P_{sx}+F_x ,$$

$$\frac{\partial v}{\partial t}+u\frac{\partial v}{\partial x}+v\frac{\partial v}{\partial y}+w\frac{\partial v}{\partial z}+fu = P_{sy}+F_y ,$$

(2)

where u, v, and w represent the velocity components in the horizontal (x and y) and vertical (s) directions, respectively, D and r_0 mean a total depth and reference density, respectively, F_x and F_y are the turbulent diffusion terms of the momentum in the horizontal direction and f denotes the Colioris parameter. P_{sx} and P_{sy} in Eq. 2 mean the hydrostatic pressure gradients in x and y directions, respectively, as expressed in the form

$$P_{sx} = -g\frac{\partial h}{\partial x}-\frac{gD}{r_0}\int_s^0\frac{\partial r'}{\partial x}ds+\frac{g}{r_0}\int_s^0 s\frac{\partial D}{\partial x}\frac{\partial r'}{\partial s}ds$$
$$P_{sy} = -g\frac{\partial h}{\partial y}-\frac{gD}{r_0}\int_s^0\frac{\partial r'}{\partial y}ds+\frac{g}{r_0}\int_s^0 s\frac{\partial D}{\partial y}\frac{\partial r'}{\partial s}ds$$

(3)

where r' means a density anomaly defined as in situ density minus the reference density r_0 and g denotes the gravitational acceleration.

In the non-hydrostatic model, we evaluate the horizontal and vertical components of the velocity, u, v and w with the horizontal and vertical momentum equations, respectively, given as

$$\frac{\partial u}{\partial t}+u\frac{\partial u}{\partial x}+v\frac{\partial u}{\partial y}+w\frac{\partial u}{\partial z}-fv = -\frac{1}{r_0}\left(\frac{\partial p_d}{\partial x}+\frac{\partial p_d}{\partial s}\frac{\partial s}{\partial x}\right)+P_{sx}+F_x ,$$

$$\frac{\partial v}{\partial t}+u\frac{\partial v}{\partial x}+v\frac{\partial v}{\partial y}+w\frac{\partial v}{\partial z}+fu = -\frac{1}{r_0}\left(\frac{\partial p_d}{\partial y}+\frac{\partial p_d}{\partial s}\frac{\partial s}{\partial y}\right)+P_{sy}+F_y ,$$ (4)

$$\frac{\partial w'}{\partial t}+u\frac{\partial w'}{\partial x}+v\frac{\partial w'}{\partial y}+\frac{w}{D}\frac{\partial w'}{\partial s} = -\frac{1}{r_0}\frac{1}{D}\frac{\partial p_d}{\partial s}+F_s ,$$

where F_s is the turbulent diffusion term of the momentum in s direction and w' is defined as

$$w' = w-D\left(\frac{\partial s}{\partial t}+u\frac{\partial s}{\partial x}+v\frac{\partial s}{\partial y}\right).$$ (5)

We compute the hydrodynamic pressure using the Poisson equation, which is derived with the continuity equation.

In computing the density, we use the conservation of the density difference r' in both the models to reduce truncation errors in the computations. The equation for the density anomaly r' is

$$\frac{\partial r'}{\partial t}+u\frac{\partial r'}{\partial x}+v\frac{\partial r'}{\partial y}+\frac{w}{D}\frac{\partial r'}{\partial s} = F_{r'} ,$$ (6)

where $F_{r'}$ represents the turbulent diffusion term of the density anomaly.

The above governing equations are computed with a finite difference method. We use here 3rd order upwind and 2nd order central differences for the advection term and the other spatial derivative
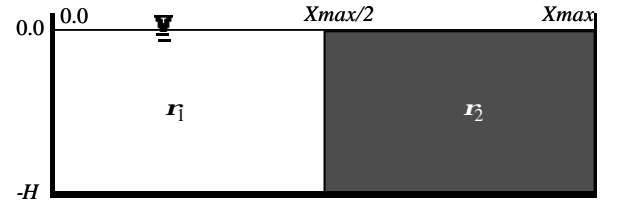
Fig. 1 Initial density distribution for the numerical simulation of a lock exchange problem.

Table 1 Computational conditions.

	Case 1	Case 2
$Xmax$	1.0 m	400.0 m
H	0.155 m	10.0 m
r_1	1000.0 kg/m³	1000.0 kg/m³
r_2	1033.0 kg/m³	1005.0 kg/m³
$\Delta x/H$	1/15.5	1/10, 1/5, 2/5, 1/2, 4/5 1.0, 1.6, 2.0, 2.5, 4.0
$\Delta z/H$	1/30	1/20, 1/15, 1/10

terms, respectively. A fractional step method (Cholin, 1968) is applied in the computation with the non-hydrodynamic model, in which the hydrodynamic pressure is calculated simultaneously with the velocities.

COMPUTATION OF A 2-D VERTICAL GRAVITY FRONT

Computational conditions

To investigate widely the influences of the hydrostatic approximation on coastal current simulations, we have performed the computation for a lock exchange problem (Turner, 1973), as a representative example of vertical 2-D gravity front problems. In the computation, two water columns with different densities are initially divided with a water gate in the center of a rectangular computational region as shown in **Fig. 1** and, after the water gate has been opened, the water masses with relatively lower and higher density flow out along surface and bottom boundaries, respectively.

Table 1 represents two computational conditions for the lock exchange problem. The first condition in the table (case1) is in line with the condition of a laboratory experiment done by Akahori et al. (1999) who studied dynamic evolution of density fronts in the lock exchange problem. In the computation for case1, we may check the numerical accuracy of the present numerical model through the comparison of the computational and experimental results. We also clarify the fundamental features of density-front structures computed with the hydrostatic and non-hydrostatic models. The condition of case2 is used to investigate how grid resolutions affect on computational accuracy of the hydrostatic and non-hydrostatic models. The Coliolis parameter f is set to be zero for simplicity.

We apply logarithmic law and slip conditions at the bottom and surface boundaries, while a slip-wall condition is employed at the other boundaries. At the initial condition, the density distribution is

(a) Non-hydrostatic model

(b) Hydrostatic model
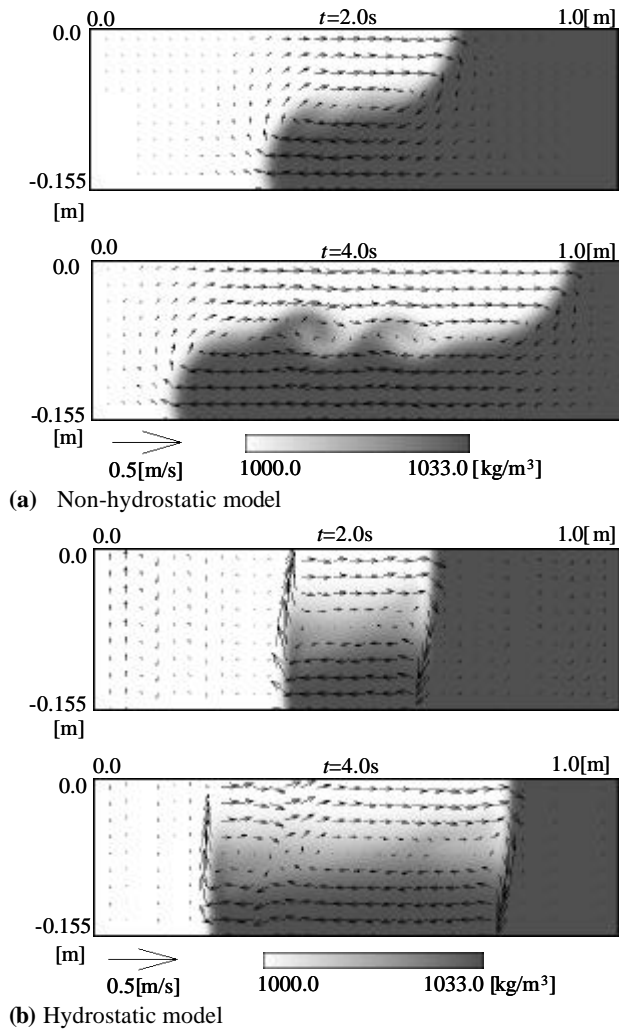
Fig. 2 Computational results of front structures in case1.

imposed as shown in **Fig.1** and a still water condition is assumed.

Fundamental features of front structures computed with both the models

To show the differences of the computational results of front structures in the hydrostatic and non-hydrostatic models, the instantaneous velocity vectors and the density distributions at t=2.0s and 4.0s in the computation for case1 are indicated in **Fig. 2** The computational results of the non-hydrostatic model, as shown in **Fig. 2(a)**, reveal that, at t=2.0s, the rounded fronts proceed horizontally along the surface and bottom boundaries and then, at t=4.0s, distinct large eddies appear near the interface between upper and lower layers, causing a vertical mixing of the density between both the layers. These front structures and large eddy motions near the interface computed with the non-hydrostatic model give acceptable agreements with those obtained by the laboratory experiment (Akahori et al., 1999), demonstrating the fundamental validity of the present numerical model.

The computational results of the hydrostatic model, as depicted in **Fig. 2(b)**, represent that the vertical velocities appear noticeably near the fronts and the corresponding front structures become much steeper. The strong vertical currents also cause the appreciable vertical mixing

of the density behind the fronts. These differences of the front structures in the computational results with the hydrostatic and non-hydrostatic models demonstrate that the hydrostatic approximation affects considerably on the computational results of the density fronts and hence may decrease the computational performance in coastal current simulations.

Influences of grid resolutions on computational accuracy

Although the computational results in the hydrostatic model are markedly different with those in the non-hydrostatic model as described in the above, these differences are influenced with a grid resolution in numerical simulations (Kinoshita, 2001). To clarify the quantitative and detailed dependence of the grid resolution on the numerical accuracy of each model, we have performed the computation for case2, in which we change the computational grid sizes widely as shown in **Table 1 Figure 3** illustrates the front structures at t=200s in the computations where three different horizontal grid resolutions ($\Delta x/H$ = 0.1, 1.0 and 2.0) are used with the finest vertical grid resolution ($\Delta z/H$ =1/20). In the case with the finest resolution ($\Delta x/H$ = 0.1), the computed front structures in both the models are qualitatively similar to those in case1. It is evident from the figure that, as the horizontal grid size increases, the differences of the computed front structure in the hydrostatic and non-hydrostatic models reduce remarkably; the non-hydrostatic model may not express the front structure sharply in lower horizontal grid resolution. On the other hand, the hydrostatic model describes more rounded front structures without strong vertical velocities near the front in the case of relatively coarser horizontal grid resolution. It should be also noted that the speed of the front evolution is slower in each model as the horizontal grid resolution is lower.

To investigate the dependence of vertical grid resolutions on the computational performance, **Fig. 4** indicates the computational results of the front structures in the computations with two different vertical grid resolutions ($\Delta z/H$ =1/15 and 1/10) at t=200s. The horizontal grid resolution is set at $\Delta x/H$ = 0.1 here. From the figure and the upper figure in **Figs. 3(a) & 3(b)**, it is apparent that although the locations of density fronts are not different in these computations, the vertical mixing of the density are more dominant as the vertical grid size become larger. We can also find from these results that in the non-hydrostatic model with the lowest vertical grid resolution ($\Delta z/H$ =1/10), a series of large eddies does not appear near the interface between upper and lower layers.

To compare quantitatively the performance of the hydrostatic and non-hydrostatic models, we shall evaluate the speed of the front evolution, which is given experimentally by Turner (1973) as

$$U_e = 0.44\sqrt{g'H} \ , \tag{7}$$

where U_e denotes the experimental front speed, H is the water depth and g' means the reduced gravity ($g' = eg$, $e = \Delta r/r_0$). **Figure 5** depicts the computed front speed U_c normalized with the experimental front speed U_e, indicating that the normalized front speed in both the models decreases as the horizontal grid size increases, and furthermore this reduction of the numerical accuracy become larger in the non-hydrostatic model than in the hydrostatic model. It is noteworthy that the vertical grid size may not influence considerably the computational accuracy for the front speed, being accordance with the results of the front structure as shown in **Fig.4**.

To examine the cause of this dependence of the horizontal grid resolution on the computational accuracy for the front speed as described above, we shall pay attention to the hydrodynamic pressure

$\Delta x/H = 0.1$

$\Delta x/H = 1.0$

$\Delta x/H = 2.0$

10m

0.5m/s

20m

1000.0   1005.0 kg/m³

(a) Non-hydrostatic model

$\Delta x/H = 0.1$

$\Delta x/H = 1.0$

$\Delta x/H = 2.0$

10m

0.5m/s

20m

1000.0   1005.0 kg/m³
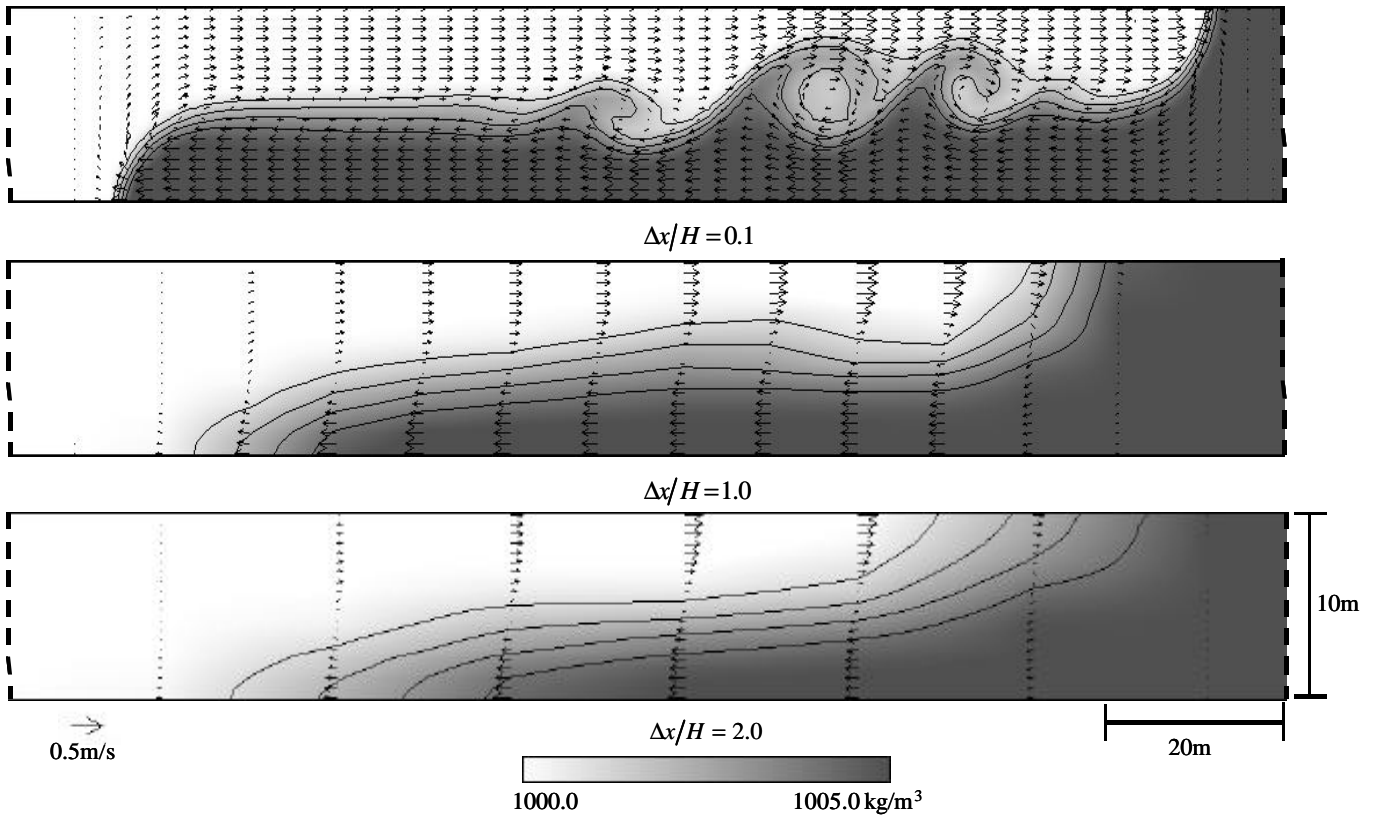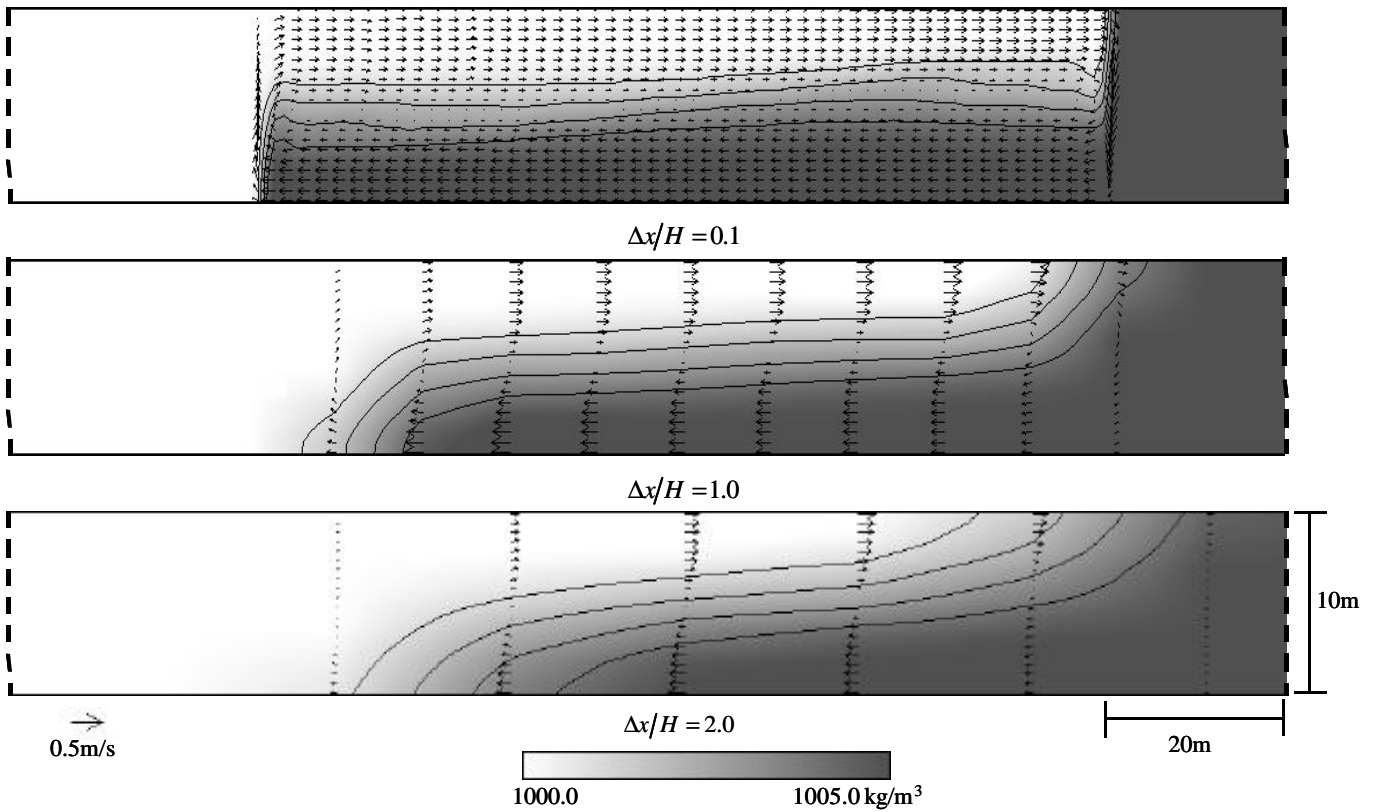
(b) Hydrostatic model

Fig.3 Influence of horizontal grid resolutions on the computational results at t=200s in case2 ($\Delta z/H$ =1/20, contour interval: 1.0kg/m³).

$\Delta z/H = 1/15$

$\Delta z/H = 1/10$

10m

20m

0.5m/s

1000.0   1005.0 kg/m³

(a) Non-hydrostatic model

$\Delta z/H = 1/15$

$\Delta z/H = 1/10$

10m

20m

0.5m/s

1000.0   1005.0 kg/m³
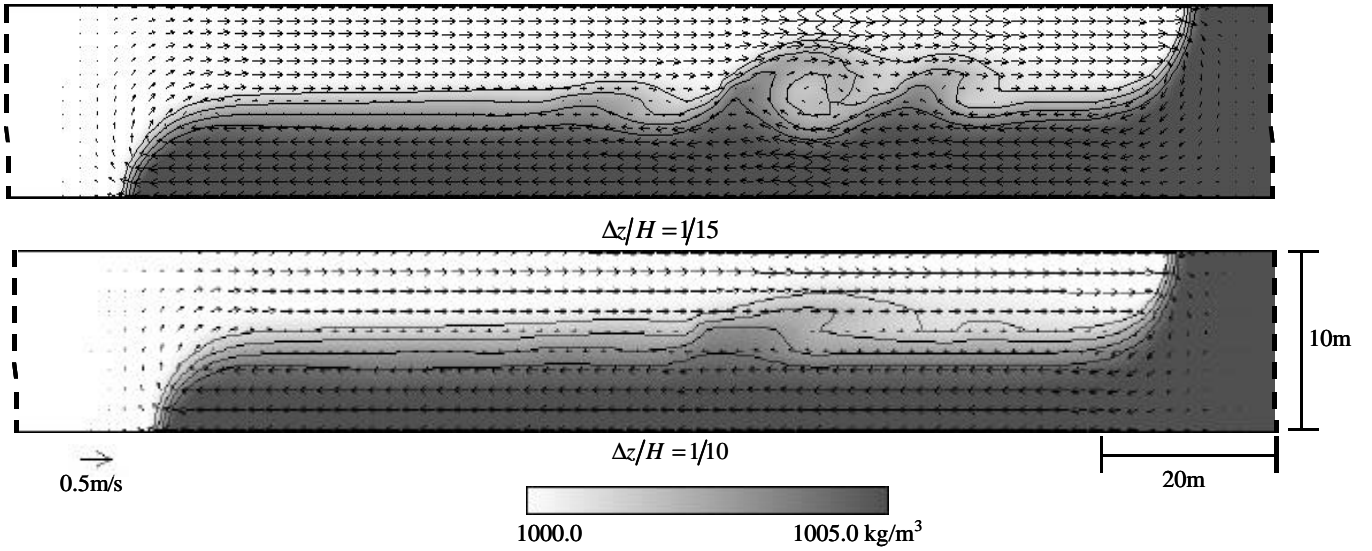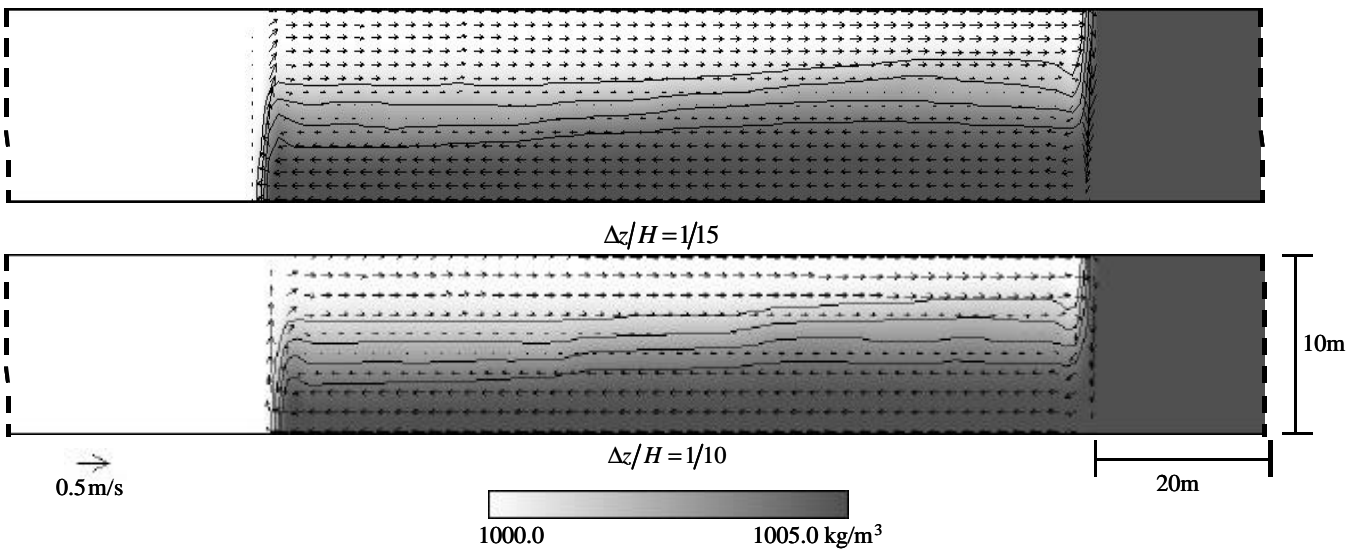
(b) Hydrostatic model

Fig.4 Influence of vertical grid sizes on the computational results at t=200s in case2 ($\Delta x/H = 0.1$, contour interval: 1.0kg/m³).
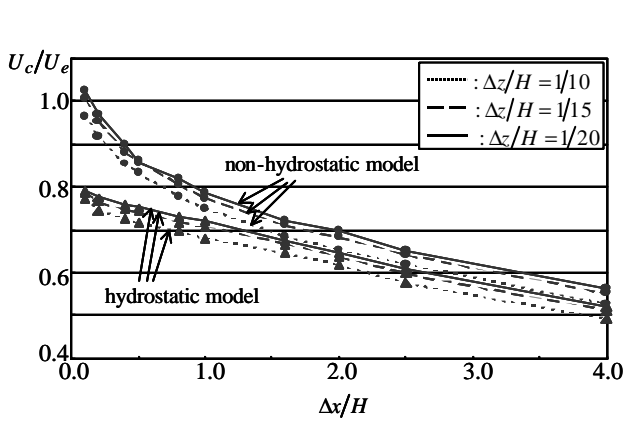
Fig.5 Normalized front speed U_c/U_e under a wide range of horizontal and vertical grid resolutions (case2, t=200s).
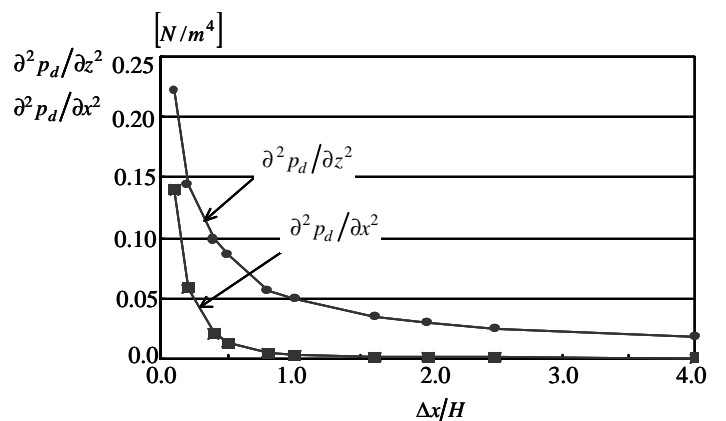
Fig.6 Numerical accuracy for the calculation of the hydrodynamic pressure P_d (case2, $\Delta z/H$ =1/20, t=300s).

P_d , which is not incorporated into the hydrostatic model. **Figure 6** indicates the second derivatives of p_d with respect to x and z, $\partial^2 p_d / \partial x^2$ and $\partial^2 p_d / \partial z^2$, which are involved in the Poisson equation. These derivative terms are spatially averaged over the whole computational domain at $t=300$s. This figure exhibits that both the terms decrease appreciably as the horizontal resolution become coarser, and the reduction becomes larger in $\partial^2 p_d / \partial x^2$ than in $\partial^2 p_d / \partial z^2$. When $\Delta x / H$ is larger than unity, $\partial^2 p_d / \partial x^2$ equals almost zero, indicating that the differences between the hydrostatic model and the non-hydrodynamic model are not clear in the relatively coarser grid resolution. These facts demonstrate that the numerical accuracy for the hydrodynamic pressure is remarkably dependent on the horizontal grid resolutions and hence the numerical accuracy of the non-hydrodynamic model decreases with the increase of the horizontal grid size due to lower performance of the calculation for the hydrodynamic pressure.

CONCLUSIONS

To investigate the influences of the hydrostatic approximation on the performance of the coastal current simulations, in the present study, we have done the numerical simulation for the lock exchange problem, one of vertical 2-D gravity fronts, under a wide range of grid resolutions. The computational results with the finest grid resolution indicate that while the non-hydrostatic model can express rounded front structures as observed in the laboratory experiment (Akahori et al., 1999), the hydrostatic model gives steeper fronts with strong vertical currents near the fronts. It is evident through the computations under various grid resolutions that the differences of the computational results in both the models become much smaller as the horizontal grid resolution become larger, indicating the crucial dependence of the horizontal grid resolutions on the computational accuracy in each model. We also clarify that the performance of the non-hydrostatic model is significantly related to the numerical accuracy for the evaluation of a hydrodynamic pressure.

REFERENCES

Akahori, R, Shimizu, Y and Nakayama, S (1999): "Numerical calculation of flow and mixing in vertical boundary surface of density," *Annual Journal of Hydraulic Engineering*, Vol.43, pp.521-527. (in Japanese)

Blumberg, AF and Mellor, GL (1983): "Diagnostic and prognostic numerical circulation studies of the south Atlantic bight", *J. Geophys. Res.*, Vol. 88, No.C8, pp.4579-4592.

Casulli, V and Stelling, GS (1999): "Numerical simulation of 3D quasi-hydrostatic free-surface flows", *Journal of Hydraulic Engineering*, Vol.24, No.7, pp.678-686.

Chorin, AJ (1968): "Numerical solution of the Navier-Stokes equations", *Math. Comput.,* Vol. 22, pp745-762.

Haidvogel, DB and Beckmann, A (1998): "Numerical models of the coastal ocean", The Sea, *John Wiley & Sons*, Vol.10, pp.457-482.

Kinoshita, T (2001): 2nd MEC Model Workshop, pp.59-63.(in Japanese)

Phillips, NA (1957): "A coordinate system having some special advantages for numerical forecasting", *J. Meteor.*, Vol.14, pp.184-185.

Turner, JS (1973): "Buoyancy effects in fluids", *Cambridge university press*, p.367.